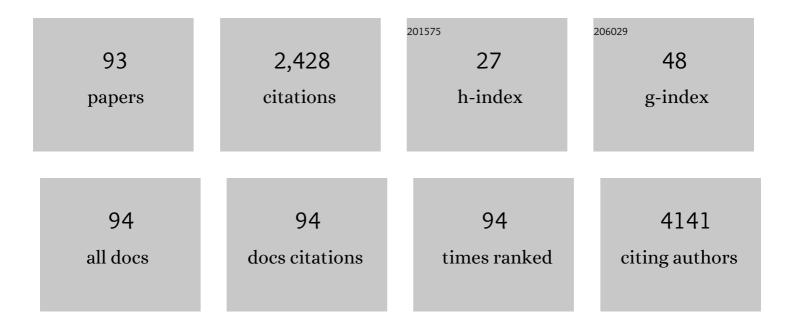
List of Publications by Year in descending order

Source: https://exaly.com/author-pdf/7050471/publications.pdf Version: 2024-02-01



Ιωρωλή Α Ηλοητεί

| # | Article | IF | CITATIONS |
|----|--|------|-----------|
| 1 | Understanding Heterogeneities in Quantum Materials. Advanced Materials, 2023, 35, e2106909. | 11.1 | 8 |
| 2 | Emergent interface vibrational structure of oxide superlattices. Nature, 2022, 601, 556-561. | 13.7 | 40 |
| 3 | Isotopes tracked on a sub-nanometre scale using electron spectroscopy. Nature, 2022, 603, 36-37. | 13.7 | Ο |
| 4 | Forecasting and modeling of the COVID-19 pandemic in the USA with a timed intervention model. Scientific Reports, 2022, 12, 4339. | 1.6 | 7 |
| 5 | Thermal Stability of Quasi-1D NbS ₃ Nanoribbons and Their Transformation to 2D NbS ₂ : Insights from <i>in Situ</i> Electron Microscopy and Spectroscopy. Chemistry of Materials, 2022, 34, 279-287. | 3.2 | 6 |
| 6 | High Throughput Data-Driven Design of Laser-Crystallized 2D MoS ₂ Chemical Sensors: A Demonstration for NO ₂ Detection. ACS Applied Nano Materials, 2022, 5, 7549-7561. | 2.4 | 5 |
| 7 | Isotope-Resolved Electron Energy Loss Spectroscopy in a Monochromated Scanning Transmission Electron Microscope. Microscopy Today, 2021, 29, 36-41. | 0.2 | 5 |
| 8 | Enhancing hyperspectral EELS analysis of complex plasmonic nanostructures with pan-sharpening. Journal of Chemical Physics, 2021, 154, 014202. | 1.2 | 5 |
| 9 | Direct visualization of anionic electrons in an electride reveals inhomogeneities. Science Advances, 2021, 7, . | 4.7 | 24 |
| 10 | Separating Physically Distinct Mechanisms in Complex Infrared Plasmonic Nanostructures via Machine Learning Enhanced Electron Energy Loss Spectroscopy. Advanced Optical Materials, 2021, 9, 2001808. | 3.6 | 13 |
| 11 | Predictability of Localized Plasmonic Responses in Nanoparticle Assemblies. Small, 2021, 17, e2100181. | 5.2 | 17 |
| 12 | Correlating inhomogeneity in anionic electron density with hydrogen incorporation in Y5Si3 electrides. Microscopy and Microanalysis, 2021, 27, 146-147. | 0.2 | 2 |
| 13 | Probing Ultralow Energy Excitations at Ultrahigh Spatial Resolution with Monochromated Electron Energy Loss Spectroscopy. Microscopy and Microanalysis, 2021, 27, 3460-3461. | 0.2 | 0 |
| 14 | Predicting local plasmon resonances and geometries using autoencoder networks in complex nanoparticle assemblies. Microscopy and Microanalysis, 2021, 27, 2766-2768. | 0.2 | 0 |
| 15 | Beyond NMF: Advanced Signal Processing and Machine Learning Methodologies for Hyperspectral Analysis in EELS. Microscopy and Microanalysis, 2021, 27, 322-324. | 0.2 | 3 |
| 16 | Revealing Nanoscale Confinement Effects on Hyperbolic Phonon Polaritons with an Electron Beam. Small, 2021, 17, e2103404. | 5.2 | 14 |
| 17 | Metalâ€Nitrogenâ€Carbon Clusterâ€Đecorated Titanium Carbide is a Durable and Inexpensive Oxygen Reduction Reaction Electrocatalyst. ChemSusChem, 2021, 14, 4680-4689. | 3.6 | 2 |
| 18 | Emerging Electron Microscopy Techniques for Probing Functional Interfaces in Energy Materials. Angewandte Chemie - International Edition, 2020, 59, 1384-1396. | 7.2 | 19 |

| # | Article | IF | CITATIONS |
|----|--|------|-----------|
| 19 | Emerging Electron Microscopy Techniques for Probing Functional Interfaces in Energy Materials. Angewandte Chemie, 2020, 132, 1400-1412. | 1.6 | 4 |
| 20 | Electroreduction of Carbon Dioxide into Selective Hydrocarbons at Low Overpotential Using Isomorphic Atomic Substitution in Copper Oxide. ACS Sustainable Chemistry and Engineering, 2020, 8, 179-189. | 3.2 | 11 |
| 21 | Cathodoluminescence Microscopies of Color Centers in Bulk and 2D Materials. Microscopy and Microanalysis, 2020, 26, 3028-3028. | 0.2 | 0 |
| 22 | Chemical and bonding analysis of liquids using liquid cell electron microscopy. MRS Bulletin, 2020, 45, 761-768. | 1.7 | 5 |
| 23 | Exploiting Electron Beam Interactions with Ultralow Energy Excitations for Nanoscale Analysis of Complex Optical and Biological Systems. Microscopy and Microanalysis, 2020, 26, 734-736. | 0.2 | 0 |
| 24 | 2D Electrets of Ultrathin MoO ₂ with Apparent Piezoelectricity. Advanced Materials, 2020, 32, e2000006. | 11.1 | 51 |
| 25 | Spectrally tunable infrared plasmonic F,Sn:In2O3 nanocrystal cubes. Journal of Chemical Physics, 2020, 152, 014709. | 1.2 | 33 |
| 26 | Ultrahigh Spatial Resolution of Mid-Infrared Optical Excitations with Monochromated Electron Energy-Loss Spectroscopy. , 2020, , . | | 0 |
| 27 | EELS in STEM: the "Swiss Army Knife―of Spectroscopy. Microscopy and Microanalysis, 2019, 25, 620-621. | 0.2 | 0 |
| 28 | A dicyanobenzoquinone based cathode material for rechargeable lithium and sodium ion batteries. Journal of Materials Chemistry A, 2019, 7, 17888-17895. | 5.2 | 35 |
| 29 | Two-Dimensional Lateral Epitaxy of 2H (MoSe ₂)–1T′ (ReSe ₂) Phases. Nano Letters, 2019, 19, 6338-6345. | 4.5 | 30 |
| 30 | Damage-Free Nanoscale Isotopic Analysis of Biological Materials with Vibrational Electron Spectroscopy. Microscopy and Microanalysis, 2019, 25, 1088-1089. | 0.2 | 0 |
| 31 | Defect-Induced Electronic Structure Changes in Cesium Lead Halide Nanocrystals. Microscopy and Microanalysis, 2019, 25, 660-661. | 0.2 | 0 |
| 32 | Etching of transition metal dichalcogenide monolayers into nanoribbon arrays. Nanoscale Horizons, 2019, 4, 689-696. | 4.1 | 11 |
| 33 | Strainâ€Induced Structural Deformation Study of 2D Mo <i>_x</i> W _{(lâ€} <i>_x</i> ₎ S ₂ . Advanced Materials Interfaces, 2019, 6, 1801262. | 1.9 | 13 |
| 34 | Identification of site-specific isotopic labels by vibrational spectroscopy in the electron microscope. Science, 2019, 363, 525-528. | 6.0 | 124 |
| 35 | Controlling the Infrared Dielectric Function through Atomic-Scale Heterostructures. ACS Nano, 2019, 13, 6730-6741. | 7.3 | 33 |
| 36 | Emergence of shallow energy levels in B-doped Q-carbon: A high-temperature superconductor. Acta Materialia, 2019, 174, 153-159. | 3.8 | 10 |

| # | Article | IF | CITATIONS |
|----|---|------|-----------|
| 37 | High-K dielectric sulfur-selenium alloys. Science Advances, 2019, 5, eaau9785. | 4.7 | 13 |
| 38 | Syntheses of Colloidal F:In ₂ O ₃ Cubes: Fluorine-Induced Faceting and Infrared Plasmonic Response. Chemistry of Materials, 2019, 31, 2661-2676. | 3.2 | 41 |
| 39 | Spatially and spectrally resolved orbital angular momentum interactions in plasmonic vortex generators. Light: Science and Applications, 2019, 8, 33. | 7.7 | 25 |
| 40 | Low Contact Barrier in 2H/1T′ MoTe ₂ In-Plane Heterostructure Synthesized by Chemical Vapor Deposition. ACS Applied Materials & Interfaces, 2019, 11, 12777-12785. | 4.0 | 70 |
| 41 | In-Situ Characterization of 2-Dim Materials at High Energy and Spatial Resolution. Microscopy and Microanalysis, 2019, 25, 17-18. | 0.2 | Ο |
| 42 | Progress in ultrahigh energy resolution EELS. Ultramicroscopy, 2019, 203, 60-67. | 0.8 | 111 |
| 43 | Atomic Structure and Electrical Activity of Grain Boundaries and Ruddlesden–Popper Faults in Cesium Lead Bromide Perovskite. Advanced Materials, 2019, 31, e1805047. | 11.1 | 72 |
| 44 | Structural Phase Transformation in Strained Monolayer MoWSe ₂ Alloy. ACS Nano, 2018, 12, 3468-3476. | 7.3 | 57 |
| 45 | Exploring the capabilities of monochromated electron energy loss spectroscopy in the infrared regime. Scientific Reports, 2018, 8, 5637. | 1.6 | 67 |
| 46 | Deformation Mechanisms of Vertically Stacked WS ₂ /MoS ₂ Heterostructures: The Role of Interfaces. ACS Nano, 2018, 12, 4036-4044. | 7.3 | 54 |
| 47 | Colossal photon bunching in quasiparticle-mediated nanodiamond cathodoluminescence. Physical Review B, 2018, 97, . | 1.1 | 26 |
| 48 | The Nanoscale Optical Properties of Complex Nanostructures. Springer Theses, 2018, , . | 0.0 | 0 |
| 49 | Elucidating Ion Transport in Lithium-Ion Conductors by Combining Vibrational Spectroscopy in STEM and Neutron Scattering. Microscopy and Microanalysis, 2018, 24, 1496-1497. | 0.2 | Ο |
| 50 | Novel EELS Experiments in the Newly Opened Monochromated Regime. Microscopy and Microanalysis, 2018, 24, 418-419. | 0.2 | 0 |
| 51 | Atomic-resolution electric field measurements with a universal detector. Microscopy and Microanalysis, 2018, 24, 114-115. | 0.2 | 1 |
| 52 | Sub-Ã…ngstrom electric field measurements on a universal detector in a scanning transmission electron microscope. Advanced Structural and Chemical Imaging, 2018, 4, 10. | 4.0 | 84 |
| 53 | Towards topological spectroscopy in the electron microscope with atomic resolution. Microscopy and Microanalysis, 2018, 24, 926-927. | 0.2 | 1 |
| 54 | Vibrational Spectroscopy of Liquid Water by Monochromated Aloof EELS. Microscopy and Microanalysis, 2018, 24, 422-423. | 0.2 | 1 |

| # | Article | IF | CITATIONS |
|----|--|------------|--------------|
| 55 | Significantly Enhanced Emission Stability of CsPbBr ₃ Nanocrystals via Chemically Induced Fusion Growth for Optoelectronic Devices. ACS Applied Nano Materials, 2018, 1, 6091-6098. | 2.4 | 42 |
| 56 | Telluride-Based Atomically Thin Layers of Ternary Two-Dimensional Transition Metal Dichalcogenide Alloys. Chemistry of Materials, 2018, 30, 7262-7268. | 3.2 | 37 |
| 57 | Thermally Induced 2D Alloyâ€Heterostructure Transformation in Quaternary Alloys. Advanced Materials, 2018, 30, e1804218. | 11.1 | 29 |
| 58 | Theoretical and Experimental Insight into the Mechanism for Spontaneous Vertical Growth of ReS 2 Nanosheets. Advanced Functional Materials, 2018, 28, 1801286. | 7.8 | 35 |
| 59 | Vibrational Spectroscopy of Water with High Spatial Resolution. Advanced Materials, 2018, 30, e1802702. | 11.1 | 45 |
| 60 | Polarization- and wavelength-resolved near-field imaging of complex plasmonic modes in Archimedean nanospirals. Optics Letters, 2018, 43, 927. | 1.7 | 13 |
| 61 | Theory-assisted determination of nano-rippling and impurities in atomic resolution images of angle-mismatched bilayer graphene. 2D Materials, 2018, 5, 041008. | 2.0 | 5 |
| 62 | Atomic-Scale Identification of Planar Defects in Cesium Lead Bromide Perovskite Nanocrystals. Microscopy and Microanalysis, 2018, 24, 100-101. | 0.2 | 2 |
| 63 | Advanced Electron Microscopy for Complex Nanotechnology. Springer Theses, 2018, , 53-74. | 0.0 | 0 |
| 64 | Extracting Interface Absorption Effects from First-Principles. Springer Theses, 2018, , 37-51. | 0.0 | 0 |
| 65 | Colossal Photon Bunching Driven by Phonon Recombination Dynamics. , 2018, , . | | 0 |
| 66 | Total Ionizing Dose Effects on Strained Ge pMOS FinFETs on Bulk Si. IEEE Transactions on Nuclear Science, 2017, 64, 226-232. | 1.2 | 28 |
| 67 | Re Doping in 2D Transition Metal Dichalcogenides as a New Route to Tailor Structural Phases and Induced Magnetism. Advanced Materials, 2017, 29, 1703754. | 11.1 | 191 |
| 68 | Memristive devices from ZnO nanowire bundles and meshes. Applied Physics Letters, 2017, 111, . | 1.5 | 11 |
| 69 | Phase Segregation Behavior of Two-Dimensional Transition Metal Dichalcogenide Binary Alloys Induced by Dissimilar Substitution. Chemistry of Materials, 2017, 29, 7431-7439. | 3.2 | 27 |
| 70 | 2D Materials: Quaternary 2D Transition Metal Dichalcogenides (TMDs) with Tunable Bandgap (Adv.) Tj ETQq0 0 (| D rgBT /Ov | erlock 10 Tf |

| 71 | Quaternary 2D Transition Metal Dichalcogenides (TMDs) with Tunable Bandgap. Advanced Materials, 2017, 29, 1702457. | 11.1 | 186 |
|----|--|------|-----|
| 72 | Observing Nanoscale Orbital Angular Momentum in Plasmon Vortices with Cathodoluminescence. Microscopy and Microanalysis, 2017, 23, 1694-1695. | 0.2 | 0 |

| # | Article | IF | CITATIONS |
|----|--|------|-----------|
| 73 | 2D Materials: Re Doping in 2D Transition Metal Dichalcogenides as a New Route to Tailor Structural Phases and Induced Magnetism (Adv. Mater. 43/2017). Advanced Materials, 2017, 29, . | 11.1 | 1 |
| 74 | Near-Field Mid-Infrared Plasmonics in Complex Nanostructures with Monochromated Electron Energy Loss Spectroscopy. Microscopy and Microanalysis, 2017, 23, 1532-1533. | 0.2 | 0 |
| 75 | Directly Identifying Phase Segregation in 2D Quaternary Alloys. Microscopy and Microanalysis, 2017, 23, 1438-1439. | 0.2 | 1 |
| 76 | Nano-chirality detection with vortex plasmon modes. , 2017, , . | | 0 |
| 77 | Colossal Bunching in Nanodiamond Cathodoluminescence. , 2017, , . | | Ο |
| 78 | Unveiling Complex Plasmonic Resonances in Archimedean Nanospirals through Cathodoluminescence in a Scanning Transmission Electron Microscope. Microscopy and Microanalysis, 2016, 22, 266-267. | 0.2 | 3 |
| 79 | Effects of Negative-Bias-Temperature-Instability on Low-Frequency Noise in SiGe \${p}\$ MOSFETs. IEEE Transactions on Device and Materials Reliability, 2016, 16, 541-548. | 1.5 | 16 |
| 80 | Probing plasmons in three dimensions by combining complementary spectroscopies in a scanning transmission electron microscope. Nanotechnology, 2016, 27, 155202. | 1.3 | 5 |
| 81 | Gold nanotriangles decorated with superparamagnetic iron oxide nanoparticles: a compositional and microstructural study. Faraday Discussions, 2016, 191, 215-227. | 1.6 | 20 |
| 82 | Quantitative first-principles theory of interface absorption in multilayer heterostructures. Applied Physics Letters, 2015, 107, 091908. | 1.5 | 3 |
| 83 | Direct Observation of Plasmonic Enhancement of Emission in Ag-nanoparticle-decorated ZnO nanostructures. Microscopy and Microanalysis, 2015, 21, 2389-2390. | 0.2 | 0 |
| 84 | Probing Plasmons in Three Dimensions within Random Morphology Nanostructures. Microscopy and Microanalysis, 2015, 21, 1683-1684. | 0.2 | 0 |
| 85 | Total Ionizing Dose Effects on Ge Channel ⁢formula formulatype= Inline >⁢tex Notation="TeX">\$p\$FETs with Raised <formula formulatype="inline"><tex notation="TeX">\${m Si}_{0.55}{m Ge}_{0.45}\$</tex> Source/Drain. IEEE Transactions on Nuclear Science, 2015, 62,</formula | 1.2 | 7 |
| 86 | Magnetic gold nanotriangles by microwave-assisted polyol synthesis. Nanoscale, 2015, 7, 14039-14046. | 2.8 | 39 |
| 87 | Spatially-Resolved, Three-Dimensional Investigation of Surface Plasmon Resonances in Complex Nanostructures. , 2015, , . | | Ο |
| 88 | Activation Energies for Oxide- and Interface-Trap Charge Generation Due to Negative-Bias Temperature Stress of Si-Capped SiGe-pMOSFETs. IEEE Transactions on Device and Materials Reliability, 2015, 15, 352-358. | 1.5 | 9 |
| 89 | The Physics of the B Factories. European Physical Journal C, 2014, 74, 1. | 1.4 | 292 |
| 90 | Bias Dependence of Total Ionizing Dose Effects in SiGe-MOS FinFETs <formula formulatype="inline"> <tex notation="TeX"></tex> . IEEE Transactions on Nuclear Science, 2014, 61, 2834-2838.</formula | 1.2 | 57 |

| # | Article | IF | CITATIONS |
|----|--|-----|-----------|
| 91 | The BB detector: Upgrades, operation and performance. Nuclear Instruments and Methods in Physics Research, Section A: Accelerators, Spectrometers, Detectors and Associated Equipment, 2013, 729, 615-701. | 0.7 | 148 |
| 92 | Observation ofB+→ηï+and search forB0decays toη′η,ηï€0,η′ï€0, andï‰ï€0. Physical Review D, 2008, 78, . | 1.6 | 11 |
| 93 | Search for neutralB-meson decays toa0ï€,a0K,î·ï0, andî·f0. Physical Review D, 2007, 75, . | 1.6 | 11 |